

Using Disorder to Identify Bogoliubov Fermi-Surface States

Hanbit Oh,¹ Daniel F. Agterberg^{2,*} and Eun-Gook Moon^{1,†}¹Department of Physics, Korea Advanced Institute of Science and Technology, Daejeon 305-701, Korea²Department of Physics, University of Wisconsin, Milwaukee, Wisconsin 53201, USA

(Received 2 June 2021; accepted 16 November 2021; published 17 December 2021)

We argue that a superconducting state with a Fermi surface of Bogoliubov quasiparticles, a Bogoliubov Fermi surface (BG-FS), can be identified by the dependence of physical quantities on disorder. In particular, we show that a linear dependence of the residual density of states at weak disorder distinguishes a BG-FS state from other nodal superconducting states. We further demonstrate the stability of supercurrent against impurities and a characteristic Drude-like behavior of the optical conductivity. Our results can be directly applied to electron irradiation experiments on candidate materials of BG-FSs, including Sr₂RuO₄, FeSe_{1-x}S_x, and UBe₁₃.

DOI: 10.1103/PhysRevLett.127.257002

Introduction.—Elucidating the role of disorder on interacting quantum many body systems has been a central issue in strongly correlated physics, as manifested in the recent advances in quantum scrambling physics [1–6]. One important class of interacting systems is strong spin-orbit coupled systems with angular momentum $j = 3/2$ [7–11]. A quadratic band touching at the Gamma point in the Brillouin zone naturally hosts a large density of states (DOS), and interaction and disorder effects are significantly enhanced [12–17]. Not only interesting normal states but also novel superconducting states are predicted [18–32]. In addition to the traditional gap structures with a full gap, a point-nodal gap, and a line-nodal gap, a Fermi surface of Bogoliubov (BG) quasiparticles in a superconducting state, a so-called Bogoliubov Fermi surface (BG-FS) [19,33–36] has been demonstrated. It has been shown that a BG-FS is topologically protected by a Z_2 invariant in centrosymmetric systems with broken time-reversal symmetry [37]. Recently, the role of interactions on such BG-FS has been considered, where it has been shown that such BG-FS states can undergo an instability to a noncentrosymmetric state [38–40]. It is confirmed that a BG-FS may still survive even with an inversion instability [38,41]. There have been several candidate materials, including heavy-fermion systems (URu₂Si₂, UBe₁₃), strontium-based compounds (Sr₂RuO₄, SrPtAs), and doped iron-based superconductors (FeSe_{1-x}S_x), but the existence of a BG-FS has not been demonstrated yet [34,35,42–52].

In the previous literature, several ideas to detect a BG-FS have been suggested, focusing on the presence of a finite nonzero DOS at zero energy in the clean limit. This can be detected through the temperature dependence of single-particle observables such as specific heat or penetration depth. However, the properties associated with a nonzero DOS cannot confirm the existence of a BG-FS because line-nodal systems with even infinitesimally low disorder

may induce a nonzero DOS [53,54]. Thus, it is highly desired to account for disorder effects on BG-FSs.

In this work, we investigate the role of disorder on a BG-FS and demonstrate that a unique signature allows a BG-FS to be identified from other nodal superconducting states. In particular, we show that a linear behavior of the residual DOS upon changing disorder and a finite superfluid density are necessary and sufficient conditions of the existence of a BG-FS. These can be measured by experiments, for example, via electron irradiation experiments. We calculate the optical conductivity [55,56] which is a powerful tool to learn the nature of the superconducting pairing gap even in the presence of disorder. Our work reconciles the role of disorder on various superconducting states with different dimensionality of zero-energy excitations and provides a new perspective on realizing exotic superconductivity.

Model.—We consider a model Hamiltonian of a BG-FS. The total Bogoliubov–de Gennes (BdG) Hamiltonian is given by

$$\mathcal{H}_0(\vec{k}) = \begin{pmatrix} H_N(\vec{k}) & \Delta(\vec{k}) \\ \Delta^\dagger(\vec{k}) & -H_N^T(-\vec{k}) \end{pmatrix}, \quad (1)$$

where $\Psi_{\vec{k}}^T \equiv (\psi_{\vec{k}}^T, \psi_{-\vec{k}}^\dagger)$ is a eight-component Nambu spinor, and $\psi_{\vec{k}}^T = (c_{\vec{k},\frac{3}{2}}, c_{\vec{k},\frac{1}{2}}, c_{\vec{k},-\frac{1}{2}}, c_{\vec{k},-\frac{3}{2}})$ is a four-component $j = 3/2$ spinor. For clarity, we choose a standard Hamiltonian introduced in the previous literature [19]. The kinetic part is described by the so-called, Luttinger Hamiltonian,

$$H_N(\vec{k}) = g_{ij} k^i k^j - \mu, \quad (2)$$

with

$$g_{ij} = \frac{\hbar^2}{2m} \left[\tilde{c}_0 \delta_{ij} + \sum_{a=1}^3 \tilde{c}_1 \Lambda_{ij}^a \gamma_a + \sum_{a=4}^5 \tilde{c}_2 \Lambda_{ij}^a \gamma_a \right]. \quad (3)$$

The 3×3 Gell-Mann matrices (Λ^a) and 4×4 Gamma matrices (γ_a) whose explicit forms are introduced in the Supplemental Material [57]. Three dimensionless parameters ($\tilde{c}_0, \tilde{c}_1, \tilde{c}_2$) are used with the chemical potential (μ) and the effective mass (m). For pairing, a chiral time-reversal symmetry breaking (TRSB) pairing is chosen,

$$\Delta(\vec{k}) = \Delta_0 [\Gamma_1 + i\Gamma_2], \quad (4)$$

where the overall pairing amplitude Δ_0 is fixed as a real number and the pairing matrices $\Gamma_a = \gamma_a U_T$ are introduced with a 4×4 antisymmetric matrix $U_T = \gamma_3 \gamma_1$. For numerical evaluation, we set $\tilde{c}_0 = 0$, $\tilde{c}_1 = \tilde{c}_2 = m = \mu = 1$, where $SO(3)$ symmetry is realized in the normal Fermi surface. Hereafter, our discussion is based on the above microscopic Hamiltonian unless otherwise stated.

The contours of zero-energy states form a toroid and spheroids in momentum space. For $\Delta_0 \neq 0$, the DOS of clean BG-FSs $D(E)$ follows the scaling relation, $D(0) \propto |\Delta_0|$ and $D(E) - D(0) \propto E^2$ in the low energy limit. Details on the zero-energy manifold and DOS are explained in the Supplemental Material [57].

Disorder and residual density of states.—We consider nonmagnetic impurities at randomly distributed positions, \vec{r}_a . Assuming $SO(3)$ rotational symmetry, the momentum-dependent disorder potential is

$$H_{\text{dis}} = \sum_{a=1}^{N_{\text{imp}}} \int_{\vec{k}, \vec{k}'} e^{i(\vec{k}' - \vec{k}) \cdot \vec{r}_a} [\psi_{\vec{k}}^\dagger V_{\text{dis}}(\hat{k}, \hat{k}') \psi_{\vec{k}'}], \quad (5)$$

with

$$V_{\text{dis}}(\hat{k}, \hat{k}') = \sum_{l=0}^{\infty} V_l P_l(\hat{k} \cdot \hat{k}'),$$

where N_{imp} is the number of identical impurities, V_l is an impurity scattering amplitude. Hereafter, the short-hand notation, $\int_{\vec{k}} \equiv \int [d^3 k / (2\pi)^3] = (1/\mathcal{V}) \sum_{\vec{k}}$, is used with a volume of a three-dimensional system \mathcal{V} . The Legendre polynomials (P_l) capture the angular dependence on the Fermi-surface with an angular momentum quantum number (l). After performing the disorder-average, translation invariance is restored and the Green's function of the disordered BG-FS is modified as, $\mathcal{G}_{\text{dis}}^{-1}(\vec{k}, i\omega) = \mathcal{G}_0^{-1}(\vec{k}, i\omega) - \Sigma_{\text{dis}}(\vec{k}, i\omega)$, where $\mathcal{G}_0^{-1}(\vec{k}, i\omega) = i\omega - \mathcal{H}_0(\vec{k})$ is the original Green's function and $\Sigma_{\text{dis}}(\vec{k}, i\omega)$ is the disordered self-energy. In the following, we consider the case with $l = 0$ as a proof of concept and consider a dilute limit of disorder, the so-called Born limit.

Employing the first order Born approximation, the scalar channel contribution to the self-energy is

$$\Sigma_{\text{dis}}(i\omega) = \frac{r_0}{8} \int_{\vec{k}} \text{Tr}[\mathcal{G}_0(\vec{k}, i\omega)], \quad (6)$$

with two parameters, $r_0 \equiv n_{\text{imp}} V_0^2$, $n_{\text{imp}} \equiv N_{\text{imp}}/\mathcal{V}$. Note that all channels other than the scalar channel may be neglected and absorbed into the changes of microscopic parameters. The imaginary part of the self-energy gives the scattering rate, $\Gamma_{\text{dis}}(E + i\eta) = -\text{Im}\Sigma_{\text{dis}}(E + i\eta) = (r_0/8)\pi D(E)$, via analytic continuation with an infinitesimal convergence parameter, $\eta > 0$. It is evident that there is a nonzero scattering rate, $\Gamma \equiv \Gamma_{\text{dis}}(i\eta) > 0$, at zero frequency, as a consequence of the nonzero DOS of a BG-FS. The scattering rate needs not be solved self-consistently in contrast to superconductors with line nodal gaps where self-consistent calculations are essential. The disorder averaged spectral function, $A_{\text{dis}}(\vec{k}, E) = [\mathcal{G}_{\text{dis}}(\vec{k}, E + i\eta) - \mathcal{G}_{\text{dis}}(\vec{k}, E - i\eta)]/2i$, gives the DOS with disorder scattering potentials,

$$D_{\text{dis}}(E; \Gamma) = -\frac{1}{\pi} \int_{\vec{k}} \text{Tr}[A_{\text{dis}}(\vec{k}, E)], \quad (7)$$

as a function of a scattering rate (Γ). The residual DOS is then defined as a difference between the DOS of dirty and clean systems, $\delta D_{\text{dis}}(\Gamma) = D_{\text{dis}}(0; \Gamma) - D(0)$.

In Fig. 1, we contrast the residual DOS of a BG-FS with that of superconductors with different nodal structures. The

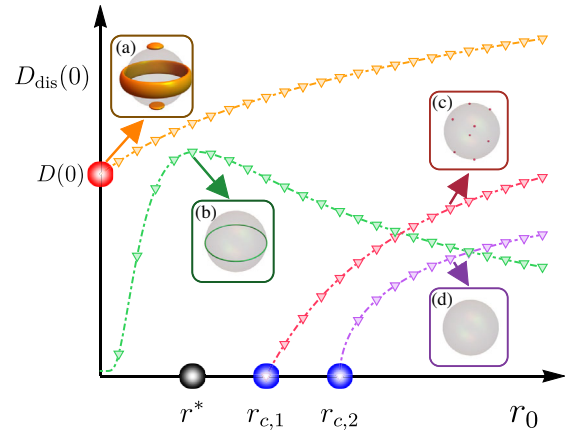


FIG. 1. Schematic DOS plot at zero energy [$D_{\text{dis}}(0)$] with various nodal superconductors as a function of impurity strength, $r_0 = n_{\text{imp}} V_0^2$. The insets show zero-energy excitations in the momentum space of four different states, BG-FS (a), line-nodal (b), point-nodal (c), and fully gapped (d) superconductors. The linear dependence of DOS on r_0 is a distinctive property of a BG-FS. Here, r^* is a resonant impurity strength for a line-nodal superconductor [53] and ($r_{c,1}, r_{c,2}$) are critical values of r_0 for point-nodal and fully gapped superconductors, respectively (see Supplemental Material [57]). The functional forms of $\delta D_{\text{dis}}(0; r_0) = D_{\text{dis}}(0; r_0) - D(0)$ are tabulated in Table I.

TABLE I. Disorder dependence of physical quantities for different nodal superconducting states: (A) BG-FS, (B) line-nodal, (C) point-nodal, and (D) fully gapped superconductors. (E) is for normal metals. The functional form, $\delta D_{\text{dis}}(r_0)$, superfluid density, \mathcal{D}_s , and the Drude-weight, \mathcal{D}_D , in the clean limit are illustrated.

States	$\delta D_{\text{dis}}(r_0)$	\mathcal{D}_s	\mathcal{D}_D
(A)	$\propto r_0$	○	○
(B)	$\propto \exp[-(r^*/r_0)]/r_0$	○	✗
(C)	$\propto [(1/r_{c,1}) - (1/r_0)]\theta(r_0 - r_{c,1})$	○	✗
(D)	$\propto \sqrt{(1/r_{c,2}) - (1/r_0)}\theta(r - r_{c,2})$	○	✗
(E)	$\propto r_0$	✗	○

r_0 dependence of the residual DOS is qualitatively different for the different nodal states. A few remarks are as follows. First, the residual DOS for a BG-FS shows a linear dependence on r_0 . To see this, we introduce a UV energy cutoff (Λ_{UV}), for example, the bandwidth, the DOS for a BG-FS is then approximated as

$$\delta D_{\text{dis}}(\Gamma) = \int_0^{\Lambda_{\text{UV}}} dE D(E) \left[\frac{\Gamma/\pi}{E^2 + \Gamma^2} - \delta(E) \right] = a_0 \Gamma, \quad (8)$$

at lowest order in $\Gamma/\Lambda_{\text{UV}} \ll 1$. For our choice of parameters, we find a linear increase in the residual DOS ($a_0 > 0$) on Γ . Using $\Gamma = (r_0/8)\pi D(0)$, this implies that the DOS linearly increases upon increasing r_0 . We can generalize the above discussion to a momentum-dependent disorder potential ($l > 0$) by including the angle dependent scattering rate $\Gamma(\vec{k})$ and see similar results (see Supplemental Material [57]). We remark that the sign of coefficient a_l is not universal but depends on the specific forms of band dispersion and disorder potential. Second, Eq. (8) may be generalized to systems with different nodal gap structures by considering a generic clean DOS, $D(E) \propto E^n$, this allows us to understand the significant differences in Fig. 1. To be specific, for line nodes, an infinitesimal impurity scattering may induce a zero-energy DOS which follows a nonlinear behavior, while it does not affect the DOS unless $r_0 > r_c$ for point nodes or full gaps. The formulas of DOS as a function of r_0 are tabulated in Table I and their detailed derivations are explained in the Supplemental Material [57]. Thus, we argue that the linear dependence of the residual DOS on impurity scattering is a unique property of BG-FSS. Third, the linear dependence of the residual DOS is observable in experiments, for example, in the tunneling conductance between a normal conductor and a BG-FS. Standard calculations show that the linear dependence effects are intact even at nonzero temperature, provided that temperature is sufficiently small compared to other energy scales, such as the disorder scattering rate or the Fermi energy of Bogoliubov quasiparticles (see Supplemental Material [57]).

Optical conductivity.—Let us consider disorder effects on the optical conductivity of a BG-FS. We focus on two aspects of the optical conductivity: The stability of the supercurrent and the existence of a Drude-like frequency dependence. We employ the standard linear response theory, and the real part of the optical conductivity in the spatially homogeneous limit is

$$\text{Re}\sigma^{ij}(\omega) = -\frac{\text{Im}Q^{ij}(\omega + i\eta)}{\omega} + \frac{\text{Re}Q^{ij}(0)}{\pi}\delta(\omega), \quad (9)$$

where Q^{ij} is the London response kernel. The conductivity of superconductors is decomposed into two parts. The former is called the regular part, $\sigma_{\text{reg}}^{ij}(\omega) = -\text{Im}Q^{ij}(\omega + i\eta)/\omega$, and the latter is called the singular part from the supercurrent, characterized by the superfluid weight, $\mathcal{D}_s^{ij} = \text{Re}Q^{ij}(0)/\pi$.

The current operator is decomposed as the paramagnetic (p) and diamagnetic (d) parts. In the Nambu basis ($\Psi_{\vec{k}}$), the zero-momentum current operator reads

$$J^i = \int_{\vec{k}} \Psi_{\vec{k}}^\dagger \mathcal{J}^i(\vec{k}) \Psi_{\vec{k}}, \quad \mathcal{J}^i = \mathcal{J}_p^i + \mathcal{J}_d^i, \quad (10)$$

with

$$\mathcal{J}_p^i(\vec{k}) = -2 \begin{pmatrix} g_{ij} & 0 \\ 0 & g_{ij}^T \end{pmatrix} k^j = -\partial_i \mathcal{H}_0(\vec{k}) \tau_z, \quad (11)$$

and

$$\mathcal{J}_d^i(\vec{k}) = -2 \begin{pmatrix} g_{ij} & 0 \\ 0 & -g_{ij}^T \end{pmatrix} A^j = -\partial_i \partial_j \mathcal{H}_0(\vec{k}) A^j, \quad (12)$$

where the Hartree unit ($e = \hbar = 1$) is used. The Pauli matrix (τ_z) acts on the particle-hole space and $\partial_i \equiv \partial_{k_i}$ is the derivative with respect to the momentum k^i . The explicit forms of the paramagnetic and diamagnetic contributions to the London response kernel are

$$Q_p^{ij}(i\omega_n) = T \sum_{ik_n} \int_{\vec{k}} \text{Tr}[\mathcal{G}_{\text{dis}}(\vec{k}, ik_n) \mathcal{J}_p^i \mathcal{G}_{\text{dis}}(\vec{k}, ik_n + i\omega_n) \mathcal{J}_p^j],$$

and

$$Q_d^{ij}(i\omega_n = 0) = T \sum_{ik_n} \int_{\vec{k}} \text{Tr}[\mathcal{G}_{\text{dis}}(\vec{k}, ik_n) \partial_i \partial_j \mathcal{H}_0],$$

respectively. Note that only the zero-frequency component ($i\omega_n = 0$) contributes to the diamagnetic kernel [58]. In what follows, we focus on the $(i, j) = (z, z)$ component of the conductivity under isotropic disorder ($l = 0$) at zero temperature ($T = 0$).

We first consider the singular part of the optical conductivity associated with the supercurrent. The superfluid

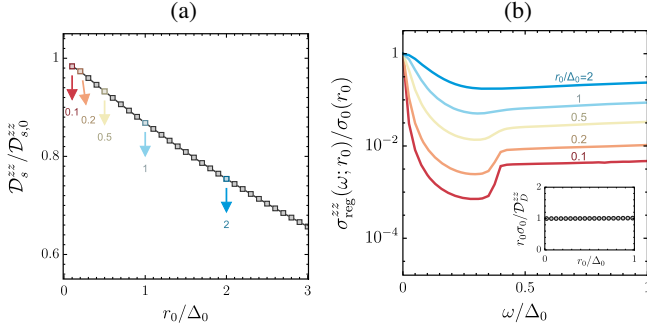


FIG. 2. (a) The r_0 dependence of the superfluid weight $\mathcal{D}_s^{zz}(r_0)$. The clean limit of the supercurrent is interpolated as a positive value, $\mathcal{D}_{s,0}^{zz} = 0.163e^2\sqrt{m\mu^3}/\hbar^3$. (b) The frequency and r_0 dependence of regular part of conductivity, $\sigma_{\text{reg}}^{zz}(\omega; r_0)$. The different values of $r_0/\Delta_0 = \{0.1, 0.2, 0.5, 1, 2\}$ are used and denoted with different colors. Inset shows $\sigma_0^{zz}(r_0) = \mathcal{D}_D^{zz}/r_0$ in the small r_0 limit with a Drude weight, $\mathcal{D}_D^{zz} = 0.168e^2\sqrt{m\mu^3}/\hbar^3$.

weight is obtained by the relation, $\mathcal{D}_s^{zz}(r_0) = \text{Re}[Q_p^{zz}(0) + Q_d^{zz}(0)]/\pi$, whose explicit form is

$$\mathcal{D}_s^{zz}(r_0) = -\frac{1}{2\pi} \int_{\vec{k}} \int_{-\infty}^{\infty} \frac{d\omega}{2\pi} \text{Tr}([\mathcal{G}_{\text{dis}}(\vec{k}, i\omega) \mathcal{J}_p^z(\vec{k}, \tau_z)^2].$$

The commutator in the integrand indicates that $\mathcal{D}_s^{zz}(r_0) = 0$ if a U(1) symmetric system is considered. In Fig. 2(a), we illustrate $\mathcal{D}_s^{zz}(r_0)$.

Our calculations indicate that the supercurrent still survives under weak disorder in a BG-FS. We note that in contrast to the previous results without disorder, our calculations converge even at $T = 0$ due to the scattering rate of the Green's function. In the clean limit ($r_0 \rightarrow 0$), the superfluid density ($\mathcal{D}_{s,0}^{zz} = 0.163e^2\sqrt{m\mu^3}/\hbar^3$) interpolates to a nonzero positive value, which shows the stability of the supercurrent under disorder and temperature. These results indicate that the supercurrent survives even with the instability associated with the inversion symmetry breaking in a centrosymmetric BG-FS. The superfluid density is naturally suppressed by increasing r_0 , similar to superconducting states with different nodal structures [59,60]. We stress that the presence of a Fermi surface of Bogoliubov quasiparticles cannot destroy the supercurrent in contrast to the Landau damping of bosonic excitations in metals.

Next, we calculate the regular part of the optical conductivity of a BG-FS. After analytic continuation, we find

$$\sigma_{\text{reg}}^{zz}(\omega; r_0) = \frac{1}{\omega} \int_{\vec{k}} \int_{-\omega}^{\omega} \frac{d\nu}{\pi} \text{Tr}[A_{\text{dis}}(\vec{k}, \nu) \mathcal{J}_p^z A_{\text{dis}}(\vec{k}, \nu + \omega) \mathcal{J}_p^z],$$

for $\omega > 0$ and $T = 0$. Here, $A_{\text{dis}}(\vec{k}, E)$ is the disorder averaged spectral function of a BG-FS. In Fig. 2(b), $\sigma_{\text{reg}}^{zz}(\omega; r_0)$ is plotted as a function of a frequency ω

the parameter r_0 . A Drude-like behavior near zero frequency with a Lorentzian distribution is obtained, similar to that found in metals. In the zero-frequency limit, the dc conductivity, $\sigma_0^{zz}(r_0) \equiv \lim_{\omega \rightarrow 0} \sigma_{\text{reg}}^{zz}(\omega; r_0)$, becomes

$$\sigma_0^{zz}(r_0) = \frac{1}{\pi} \int_{\vec{k}} \text{Tr}[A_{\text{dis}}(\vec{k}, 0) \mathcal{J}_p^z A_{\text{dis}}(\vec{k}, 0) \mathcal{J}_p^z], \quad (13)$$

at zero temperature. Note that a nonzero dc-limit conductivity also appears in line-node superconductors, for example, d -wave superconductors [53,56,60,61], but it is not Drude-like in contrast to a BG-FS, where $\sigma_0(r_0) \propto 1/r_0$ is manifested [see inset of Fig. 2(b)]. In the clean limit, the dc conductivity of a BG-FS diverges and yields a Drude-weight, $\mathcal{D}_D^{zz} \neq 0$,

$$\lim_{r_0 \rightarrow 0} \frac{\sigma_{\text{reg}}^{zz}(\omega; r_0)}{\pi} = \mathcal{D}_D^{zz} \delta(\omega) + \dots, \quad (14)$$

where a nonsingular term is omitted in \dots . We find $\mathcal{D}_D^{zz} = 0.168e^2\sqrt{m\mu^3}/\hbar^3$ for our choice of parameters. In the Supplemental Material [57], the dc conductivity of superconducting states with various nodes and their Γ dependencies are shown. Therefore, The Drude-like behavior is a distinctive feature of a BG-FS.

Discussion and conclusion.—Our studies indicate that a BG-FS may be uniquely characterized by the dependence on disorder. Thus, we propose electron irradiation experiments can be a powerful tool to identify a BG-FS by observing the linear disorder dependence of the residual DOS and superfluid density, as summarized in Table I.

Our results are directly applicable to experiments. We believe that the candidate materials of BG-FSs such as $\text{FeSe}_{1-x}\text{S}_x$ for $x > 0.17$ [62] and Th-doped UBe_{13} [45] are promising since a likely intrinsic residual density of states has already been reported to be observed. We stress that other experiments such as heat capacity and the magneto-optical Kerr effect can be also used to observe the disorder dependence since the residual DOS appears in these observables.

Note that, for simplicity, our calculations mainly focus on the cases with a SO(3) symmetric normal band structure and non-magnetic impurity scattering at zero temperature. It is straightforward to generalize our calculations to include anisotropic and magnetic impurity scattering and we show in the Supplemental Material [57] that our main results are not modified. In particular, the robustness of a BG-FS against disorder is considered, and we prove that the Anderson theorem is violated for a BG-FS in accordance with common wisdom. Considering both arbitrary pairings and generic disorder potentials, we quantify the fragility of a superconducting state and generalize the concept of superconducting fitness function and the previous literature [63–67]. See Supplemental Material [57] for more information.

The following questions regarding a BG-FS remain to be answered in future research. The strong disorder effects on a BG-FS need to be understood. It would be interesting to clarify whether the conventional approach with the nonlinear sigma model in symmetry class D applies [68,69]. The verification of the f -sum rule on the linear conductivity of a BG-FS and the generalization to the nonlinear conductivities is also an open question [70]. We believe that our work may raise many interesting future studies and open up new directions to search for exotic superconductivity.

The authors thank Y. Bang and J. Ahn for invaluable discussions and comments. We are particularly grateful to T. Shibauchi for communicating ideas in experiments of doped FeSe. H. O. and E.-G.M. are supported by the National Research Foundation of Korea (NRF) Grants No. 2019M3E4A1080411, No. 2020R1A4A3079707, and No. 2021R1A2C4001847. D. F. A. was supported by the U.S. Department of Energy, Office of Basic Energy Sciences, Division of Materials Sciences and Engineering under Award No. DE-SC0021971.

* agterber@uwm.edu

† egmoon@kaist.ac.kr

- [1] S. Sachdev and J. Ye, *Phys. Rev. Lett.* **70**, 3339 (1993).
 [2] Y. Sekino and L. Susskind, *J. High Energy Phys.* **10** (2008) 065.
 [3] S. H. Shenker and D. Stanford, *J. High Energy Phys.* **03** (2014) 067.
 [4] J. Maldacena, S. H. Shenker, and D. Stanford, *J. High Energy Phys.* **08** (2016) 106.
 [5] P. Hosur, X.-L. Qi, D. A. Roberts, and B. Yoshida, *J. High Energy Phys.* **02** (2016) 004.
 [6] A. A. Patel, D. Chowdhury, S. Sachdev, and B. Swingle, *Phys. Rev. X* **7**, 031047 (2017).
 [7] W. Witczak-Krempa, G. Chen, Y. B. Kim, and L. Balents, *Annu. Rev. Condens. Matter Phys.* **5**, 57 (2014).
 [8] Y. Tokiwa, J. J. Ishikawa, S. Nakatsuji, and P. Gegenwart, *Nat. Mater.* **13**, 356 (2014).
 [9] T. Kondo, M. Nakayama, R. Chen, J. J. Ishikawa, E.-G. Moon, T. Yamamoto, Y. Ota, W. Malaeb, H. Kanai, Y. Nakashima, Y. Ishida, R. Yoshida, H. Yamamoto, M. Matsunami, S. Kimura, N. Inami, K. Ono, H. Kumigashira, S. Nakatsuji, L. Balents, and S. Shin, *Nat. Commun.* **6**, 10042 (2015).
 [10] Z. Tian, Y. Kohama, T. Tomita, H. Ishizuka, T. H. Hsieh, J. J. Ishikawa, K. Kindo, L. Balents, and S. Nakatsuji, *Nat. Phys.* **12**, 134 (2016).
 [11] K. Ueda, R. Kaneko, H. Ishizuka, J. Fujioka, N. Nagaosa, and Y. Tokura, *Nat. Commun.* **9**, 3032 (2018).
 [12] E.-G. Moon, C. Xu, Y. B. Kim, and L. Balents, *Phys. Rev. Lett.* **111**, 206401 (2013).
 [13] I. F. Herbut and L. Janssen, *Phys. Rev. Lett.* **113**, 106401 (2014).
 [14] H.-H. Lai, B. Roy, and P. Goswami, *arXiv:1409.8675*.
 [15] R. M. Nandkishore and S. A. Parameswaran, *Phys. Rev. B* **95**, 205106 (2017).
 [16] I. Mandal and R. M. Nandkishore, *Phys. Rev. B* **97**, 125121 (2018).
 [17] I. Mandal, *Ann. Phys. (Amsterdam)* **392**, 179 (2018).
 [18] P. M. R. Brydon, L. Wang, M. Weinert, and D. F. Agterberg, *Phys. Rev. Lett.* **116**, 177001 (2016).
 [19] D. F. Agterberg, P. M. R. Brydon, and C. Timm, *Phys. Rev. Lett.* **118**, 127001 (2017).
 [20] C. Timm, A. P. Schnyder, D. F. Agterberg, and P. M. R. Brydon, *Phys. Rev. B* **96**, 094526 (2017).
 [21] J. W. F. Venderbos, L. Savary, J. Ruhman, P. A. Lee, and L. Fu, *Phys. Rev. X* **8**, 011029 (2018).
 [22] L. Savary, J. Ruhman, J. W. F. Venderbos, L. Fu, and P. A. Lee, *Phys. Rev. B* **96**, 214514 (2017).
 [23] B. Roy, S. A. A. Ghorashi, M. S. Foster, and A. H. Nevidomskyy, *Phys. Rev. B* **99**, 054505 (2019).
 [24] Y. Nakajima, R. Hu, K. Kirshenbaum, A. Hughes, P. Syers, X. Wang, K. Wang, R. Wang, S. R. Saha, D. Pratt, J. W. Lynn, and J. Paglione, *Sci. Adv.* **1**, e1500242 (2015).
 [25] H. Kim, K. Wang, Y. Nakajima, R. Hu, S. Ziemak, P. Syers, L. Wang, H. Hodovanets, J. D. Denlinger, P. M. R. Brydon, D. F. Agterberg, M. A. Tanatar, R. Prozorov, and J. Paglione, *Sci. Adv.* **4**, eaao4513 (2018).
 [26] I. Boettcher and I. F. Herbut, *Phys. Rev. Lett.* **120**, 057002 (2018).
 [27] G. B. Sim, A. Mishra, M. J. Park, Y. B. Kim, G. Y. Cho, and S. Lee, *Phys. Rev. B* **100**, 064509 (2019).
 [28] G. B. Sim, A. Mishra, M. J. Park, Y. B. Kim, G. Y. Cho, and S. B. Lee, *Phys. Rev. Research* **2**, 023416 (2020).
 [29] S. Tchoumakov, L. J. Godbout, and W. Witczak-Krempa, *Phys. Rev. Research* **2**, 013230 (2020).
 [30] C. J. Lapp, G. Börner, and C. Timm, *Phys. Rev. B* **101**, 024505 (2020).
 [31] H. Menke, C. Timm, and P. M. R. Brydon, *Phys. Rev. B* **100**, 224505 (2019).
 [32] H. Oh, S. Lee, Y. B. Kim, and E.-G. Moon, *Phys. Rev. Lett.* **122**, 167201 (2019).
 [33] I. F. Herbut and J. M. Link, *Phys. Rev. B* **103**, 144517 (2021).
 [34] C. Setty, S. Bhattacharyya, Y. Cao, A. Kreisel, and P. J. Hirschfeld, *Nat. Commun.* **11**, 523 (2020).
 [35] C. Setty, Y. Cao, A. Kreisel, S. Bhattacharyya, and P. J. Hirschfeld, *Phys. Rev. B* **102**, 064504 (2020).
 [36] E. Berg, C.-C. Chen, and S. A. Kivelson, *Phys. Rev. Lett.* **100**, 027003 (2008).
 [37] P. M. R. Brydon, D. F. Agterberg, H. Menke, and C. Timm, *Phys. Rev. B* **98**, 224509 (2018).
 [38] H. Oh and E.-G. Moon, *Phys. Rev. B* **102**, 020501(R) (2020).
 [39] S.-T. Tamura, S. Iimura, and S. Hoshino, *Phys. Rev. B* **102**, 024505 (2020).
 [40] C. Timm, P. M. R. Brydon, and D. F. Agterberg, *Phys. Rev. B* **103**, 024521 (2021).
 [41] J. M. Link and I. F. Herbut, *Phys. Rev. Lett.* **125**, 237004 (2020).
 [42] E. R. Schemm, R. E. Baumbach, P. H. Tobash, F. Ronning, E. D. Bauer, and A. Kapitulnik, *Phys. Rev. B* **91**, 140506(R) (2015).
 [43] Y. Kasahara, T. Iwasawa, H. Shishido, T. Shibauchi, K. Behnia, Y. Haga, T. D. Matsuda, Y. Onuki, M. Sgrist, and Y. Matsuda, *Phys. Rev. Lett.* **99**, 116402 (2007).

- [44] R. H. Heffner, J. L. Smith, J. O. Willis, P. Birrer, C. Baines, F. N. Gygax, B. Hitti, E. Lippelt, H. R. Ott, A. Schenck, E. A. Knetsch, J. A. Mydosh, and D. E. MacLaughlin, *Phys. Rev. Lett.* **65**, 2816 (1990).
- [45] R. J. Zieve, R. Duke, and J. L. Smith, *Phys. Rev. B* **69**, 144503 (2004).
- [46] G. M. Luke, Y. Fudamoto, K. M. Kojima, M. I. Larkin, J. Merrin, B. Nachumi, Y. J. Uemura, Y. Maeno, Z. Q. Mao, Y. Mori, H. Nakamura, and M. Sigrist, *Nature (London)* **394**, 558 (1998).
- [47] J. Xia, Y. Maeno, P. T. Beyersdorf, M. M. Fejer, and A. Kapitulnik, *Phys. Rev. Lett.* **97**, 167002 (2006).
- [48] H. G. Suh, H. Menke, P. M. R. Brydon, C. Timm, A. Ramires, and D. F. Agterberg, *Phys. Rev. Research* **2**, 032023(R) (2020).
- [49] P. K. Biswas, H. Luetkens, T. Neupert, T. Stürzer, C. Baines, G. Pascua, A. P. Schnyder, M. H. Fischer, J. Goryo, M. R. Lees, H. Maeter, F. Brückner, H.-H. Klauss, M. Nicklas, P. J. Baker, A. D. Hillier, M. Sigrist, A. Amato, and D. Johrendt, *Phys. Rev. B* **87**, 180503(R) (2013).
- [50] Y. Sato, S. Kasahara, T. Taniguchi, X. Xing, Y. Kasahara, Y. Tokiwa, Y. Yamakawa, H. Kontani, T. Shibauchi, and Y. Matsuda, *Proc. Natl. Acad. Sci. U.S.A.* **115**, 1227 (2018).
- [51] K. Matsuura, T. Takenaka, Y. Sugimura, T. Shibauchi, K. Yamakawa, Q. Sheng, Z. Guguchia, Y. Uemura, Y. Cai, G. Luke *et al.*, in *APS March Meeting Abstracts* (2019), Vol. 2019, pp. E10–006.
- [52] N. Fujiwara, T. Kuwayama, K. Matsuura, Y. Mizukami, S. Kasahara, Y. Matsuda, T. Shibauchi, and Y. Uwatoko, in *APS March Meeting Abstracts* (2019), Vol. 2019, pp. E10–007.
- [53] A. C. Durst and P. A. Lee, *Phys. Rev. B* **62**, 1270 (2000).
- [54] M. J. Graf, S.-K. Yip, J. A. Sauls, and D. Rainer, *Phys. Rev. B* **53**, 15147 (1996).
- [55] I. Boettcher, *Phys. Rev. B* **99**, 125146 (2019).
- [56] J. Ahn and N. Nagaosa, *Nat. Commun.* **12**, 1617 (2021).
- [57] See Supplemental Material at <http://link.aps.org/supplemental/10.1103/PhysRevLett.127.257002> for further details on the Fermionic Hamiltonian, the calculation of the residual density of states, the calculation of the optical conductivity, and the role of disorder on the transition temperature.
- [58] P. Coleman, *Introduction to Many-Body Physics, Chapter 10* (Cambridge University Press, Cambridge, England, 2015).
- [59] G. Bimonte, H. Haakh, C. Henkel, and F. Intravaia, *J. Phys. A* **43**, 145304 (2010).
- [60] Y. Sun and K. Maki, *Europhys. Lett.* **32**, 355 (1995).
- [61] B. Dra, A. Virosztek, and K. Maki, *Physica (Amsterdam)* **341–348C**, 775 (2000).
- [62] T. Shibauchi, T. Hanaguri, and Y. Matsuda, *J. Phys. Soc. Jpn.* **89**, 102002 (2020).
- [63] A. Ramires and M. Sigrist, *Phys. Rev. B* **94**, 104501 (2016).
- [64] A. Ramires, D. F. Agterberg, and M. Sigrist, *Phys. Rev. B* **98**, 024501 (2018).
- [65] L. Andersen, A. Ramires, Z. Wang, T. Lorenz, and Y. Ando, *Sci. Adv.* **6** (2020).
- [66] D. C. Cavanagh and P. M. R. Brydon, *Phys. Rev. B* **101**, 054509 (2020).
- [67] D. C. Cavanagh and P. M. R. Brydon, *Phys. Rev. B* **104**, 014503 (2021).
- [68] A. Altland and B. D. Simons, *Condensed Matter Field Theory* (Cambridge University Press, Cambridge, England, 2010).
- [69] S. Ryu and K. Nomura, *Phys. Rev. B* **85**, 155138 (2012).
- [70] H. Watanabe and M. Oshikawa, *Phys. Rev. B* **102**, 165137 (2020).